

Heterogeneous & Homogeneous & Bio- & Nano-

CHEM **CAT** CHEM

CATALYSIS

Supporting Information

A Theoretical Investigation on CO Oxidation by Single-Atom Catalysts $M_1/\gamma\text{-Al}_2\text{O}_3$ ($M = \text{Pd, Fe, Co, and Ni}$)

Tao Yang,^[a, d] Ryoichi Fukuda,^[a, d] Saburo Hosokawa,^[b, d] Tsunehiro Tanaka,^[b, d]
Shigeyoshi Sakaki,^{*, [c, d]} and Masahiro Ehara^{*, [a, d]}

cctc_201601713_sm_miscellaneous_information.pdf

Contents

- I. Geometries and Electronic Properties of M_1/Al_2O_3 ($M = Pd, Fe, Co, \text{ and } Ni$)
- II. Geometries and Electronic Properties of Intermediate **2** of M_1/Al_2O_3 ($M = Pd, Fe, Co, \text{ and } Ni$)
- III. Geometries and Electronic Properties of Intermediate **4** of M_1/Al_2O_3 ($M = Pd, Fe, Co, \text{ and } Ni$)
- IV. Geometries of Transition State **5-TS** of M_1/Al_2O_3 ($M = Pd, Fe, Co, \text{ and } Ni$)
- V. Geometries of Intermediate **6** of M_1/Al_2O_3 ($M = Pd, Fe, Co, \text{ and } Ni$).
- VI. Geometries and Electronic Properties of Intermediate **8** of M_1/Al_2O_3 ($M = Pd, Fe, Co, \text{ and } Ni$)
- VII. Geometries and Electronic Properties of Intermediate **9** of M_1/Al_2O_3 ($M = Pd, Fe, Co, \text{ and } Ni$)

I. Geometries and Electronic Properties of Al_2O_3 and $\text{M}_1/\text{Al}_2\text{O}_3$ ($\text{M} = \text{Pd}, \text{Fe}, \text{Co}, \text{and Ni}$)

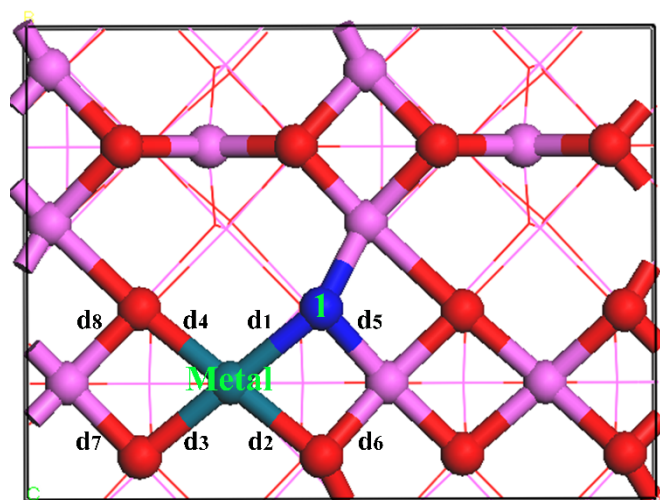


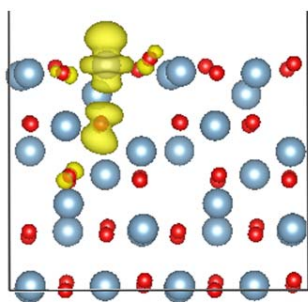
Figure S1. Geometries of $\text{M}_1/\text{Al}_2\text{O}_3$ ($\text{M} = \text{Pd}, \text{Fe}, \text{Co}, \text{and Ni}$)

Table S1. Spin state and Bader charges of the metal atom (M) and lattice oxygen (O_1) in Al_2O_3 and $\text{M}_1/\text{Al}_2\text{O}_3$ ($\text{M} = \text{Pd}, \text{Fe}, \text{Co}, \text{and Ni}$).

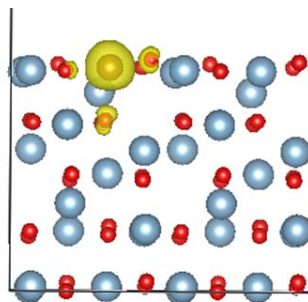
System	Spin State	Charge(M)	Charge(O_1)
		e	e
Al_2O_3	0	+2.444	-1.619
$\text{Pd}_1/\text{Al}_2\text{O}_3$	0.98	+1.074	-1.376
$\text{Fe}_1/\text{Al}_2\text{O}_3$	5.01	+1.615	-1.459
$\text{Co}_1/\text{Al}_2\text{O}_3$	4.07	+1.538	-1.421
$\text{Ni}_1/\text{Al}_2\text{O}_3$	1.10	+1.234	-1.427

Table S2. Important bond distances in Al_2O_3 and $\text{M}_1/\text{Al}_2\text{O}_3$ ($\text{M} = \text{Pd}, \text{Fe}, \text{Co}, \text{and Ni}$).

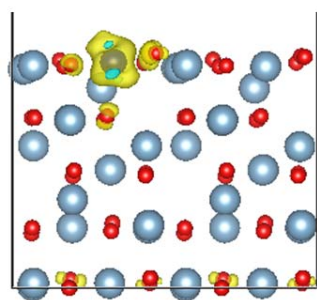
System	d_1	d_2	d_3	d_4	d_5	d_6	d_7	d_8
	Å	Å	Å	Å	Å	Å	Å	Å
Al_2O_3	1.949	1.949	1.981	1.981	1.836	1.836	1.846	1.846
$\text{Pd}_1/\text{Al}_2\text{O}_3$	2.097	2.097	2.106	2.106	1.819	1.819	1.843	1.843
$\text{Fe}_1/\text{Al}_2\text{O}_3$	2.028	2.028	2.115	2.115	1.837	1.837	1.847	1.847
$\text{Co}_1/\text{Al}_2\text{O}_3$	1.906	2.080	1.912	2.385	1.867	1.812	1.850	1.822
$\text{Ni}_1/\text{Al}_2\text{O}_3$	2.015	2.015	1.976	1.976	1.816	1.816	1.841	1.841



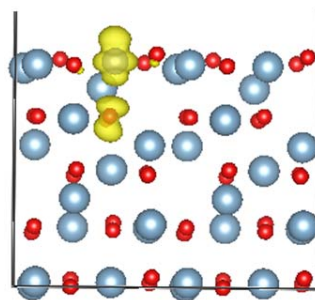
Pd



Fe



Co



Ni

Figure S2. Spin density of M₁/Al₂O₃ (M = Pd, Fe, Co and Ni).

II. Geometries and Electronic Properties of Intermediate 2 of M_1/Al_2O_3 ($M = Pd, Fe, Co, \text{ and } Ni$)

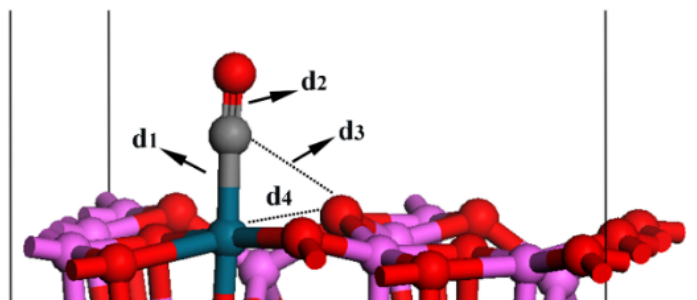


Figure S3. Geometries of intermediate 2 of M_1/Al_2O_3 ($M = Pd, Fe, Co, \text{ and } Ni$)

Table S3. Spin state (S), Bader charges of the metal atom (M), lattice oxygen (O_{lattice}), carbon (C) and oxygen (O_{co}) of CO, bond distances in intermediate 2 (shown in Figure S3).

System	S	M	O_{lattice}	C	O_{co}	d_1	d_2	d_3	d_4
		e	e	e	e	Å	Å	Å	Å
Pd_1/Al_2O_3	0.97	+1.067	-1.424	+1.130	-1.017	1.881	1.148	2.747	2.341
Fe_1/Al_2O_3	4.89	+1.621	-1.464	+1.098	-1.084	2.282	1.142	2.758	2.104
Co_1/Al_2O_3	0.00	+1.261	-1.416	+1.046	-1.059	1.750	1.153	2.615	2.059
Ni_1/Al_2O_3	0.99	+1.183	-1.459	+1.110	-1.033	1.797	1.146	2.586	2.287

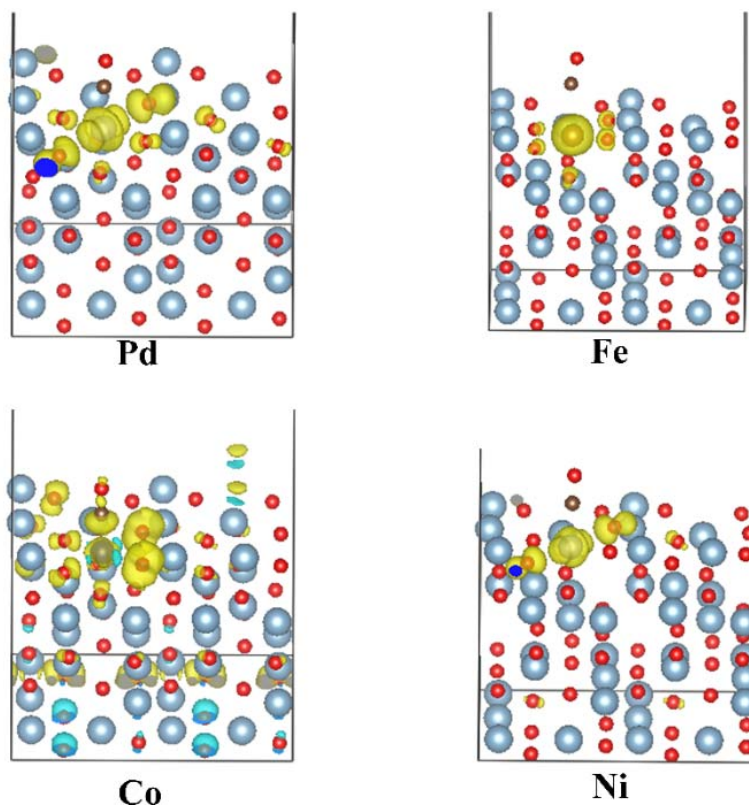


Figure S4. Spin density of intermediate 1 of M_1/Al_2O_3 ($M = Pd, Fe, Co \text{ and } Ni$). Antiferromagnetism

appears in intermediate **1** of $\text{Co}_1/\text{Al}_2\text{O}_3$.

The spin density of four single-atom catalysts are shown Figure R1. It is found that spin distribution maps of $\text{Ni}_1/\text{Al}_2\text{O}_3$ and $\text{Pd}_1/\text{Al}_2\text{O}_3$ are similar. As shown in Figure R2, the CO adsorption modifies the spin distribution of $\text{Ni}_1/\text{Al}_2\text{O}_3$ and $\text{Pd}_1/\text{Al}_2\text{O}_3$ and activates the surface O atom which has large spin density. For $\text{Fe}_1/\text{Al}_2\text{O}_3$, the weak interaction between CO and Fe doesn't affect the spin distribution. In the case of $\text{Co}_1/\text{Al}_2\text{O}_3$, the spin state is strongly influenced by the CO adsorption due to the strong interaction between CO and Co.

III. Geometries and Electronic Properties of Intermediate 4 of M_1/Al_2O_3 ($M = Pd, Fe, Co,$ and Ni)

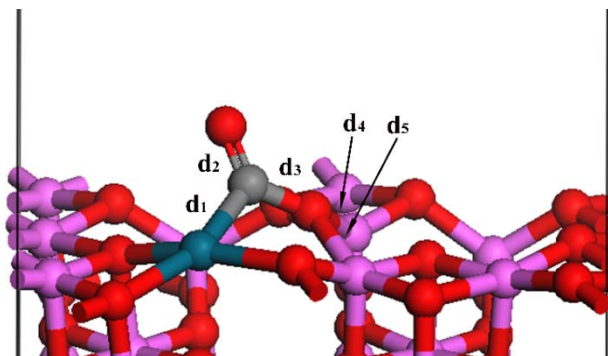


Figure S5. Geometries of intermediate **4** of M_1/Al_2O_3 ($M = Pd, Fe, Co,$ and Ni)

Table S4. Spin state (S), Bader charges of the metal atom (M), the active lattice oxygen atoms ($O_{lattice}$), carbon atom (C) and oxygen atom (O_{co}) of CO in intermediate **4**.

System	S	M e	$O_{lattice}$ e	C e	O_{co} e
Pd_1/Al_2O_3	1.00	+0.831	-1.359	+1.506	-1.053
Fe_1/Al_2O_3	3.00	+1.307	-1.347	+1.304	-1.074
Co_1/Al_2O_3	2.00	+1.138	-1.323	+1.427	-1.055
Ni_1/Al_2O_3	0.99	+1.046	-1.362	+1.479	-1.045

Table S5. Relevant distances of intermediate **4** shown in Figure S5.

System	d_1 Å	d_2 Å	d_3 Å	d_4 Å	d_5 Å
Pd_1/Al_2O_3	1.923	1.205	1.353	1.866	1.946
Fe_1/Al_2O_3	1.899	1.203	1.401	1.881	1.912
Co_1/Al_2O_3	1.876	1.200	1.367	1.964	1.935
Ni_1/Al_2O_3	1.852	1.202	1.351	1.873	1.931

IV. Geometries of Transition State 5TS of M_1/Al_2O_3 ($M = Pd, Fe, Co, \text{ and } Ni$)

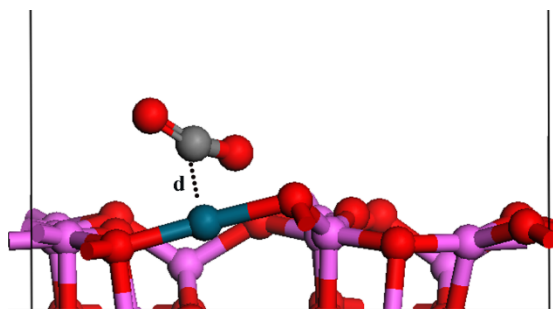


Figure S6. Geometries of transition state **5TS** of M_1/Al_2O_3 ($M = Pd, Fe, Co, \text{ and } Ni$)

Table S6. The distance between the metal atom and carbon atom of CO_2 in the transition state **5TS**.

System	d Å
Pd_1/Al_2O_3	2.324
Fe_1/Al_2O_3	2.669
Co_1/Al_2O_3	2.624
Ni_1/Al_2O_3	1.852

V. Geometries of Intermediate 6 of M_1/Al_2O_3 ($M = Pd, Fe, Co, \text{ and } Ni$)

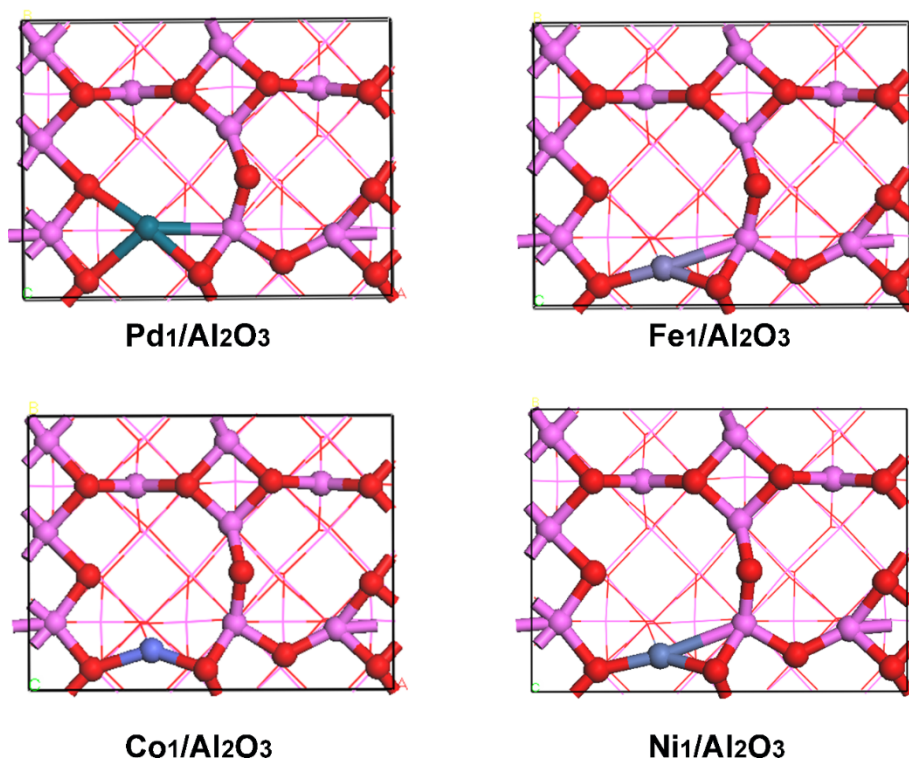


Figure S7. Geometries of intermediate **6** of M_1/Al_2O_3 ($M = Pd, Fe, Co, \text{ and } Ni$). The CO molecule has been omitted for clarity.

VI. Geometries and Electronic Properties of Intermediate **8 of M_1/Al_2O_3 ($M = Pd, Fe, Co,$ and Ni)**

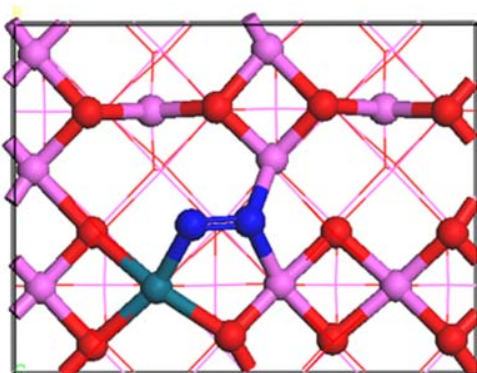


Figure S8. Geometries of intermediate **8** of M_1/Al_2O_3 ($M = Pd, Fe, Co,$ and Ni)

Table S7. Spin state (S), Bader charges of the metal atom (M) and adsorbed oxygen molecule (O_a and O_b), and bond distances between metal atom and oxygen atom as well as between oxygen and oxygen atom in intermediate **8**.

System	S	M e	O_a e	O_b e	M-O distance Å	O-O distance Å
Pd_1/Al_2O_3	0.89	+1.034	-0.326	-0.879	1.909	1.449
Fe_1/Al_2O_3	5.00	+1.559	-0.447	-0.916	1.902	1.466
Co_1/Al_2O_3	1.99	+1.295	-0.382	-0.885	1.748	1.471
Ni_1/Al_2O_3	1.02	+1.200	-0.368	-0.882	1.800	1.450

Isolated O-O bond distance in O_2 molecule: 1.236 Å

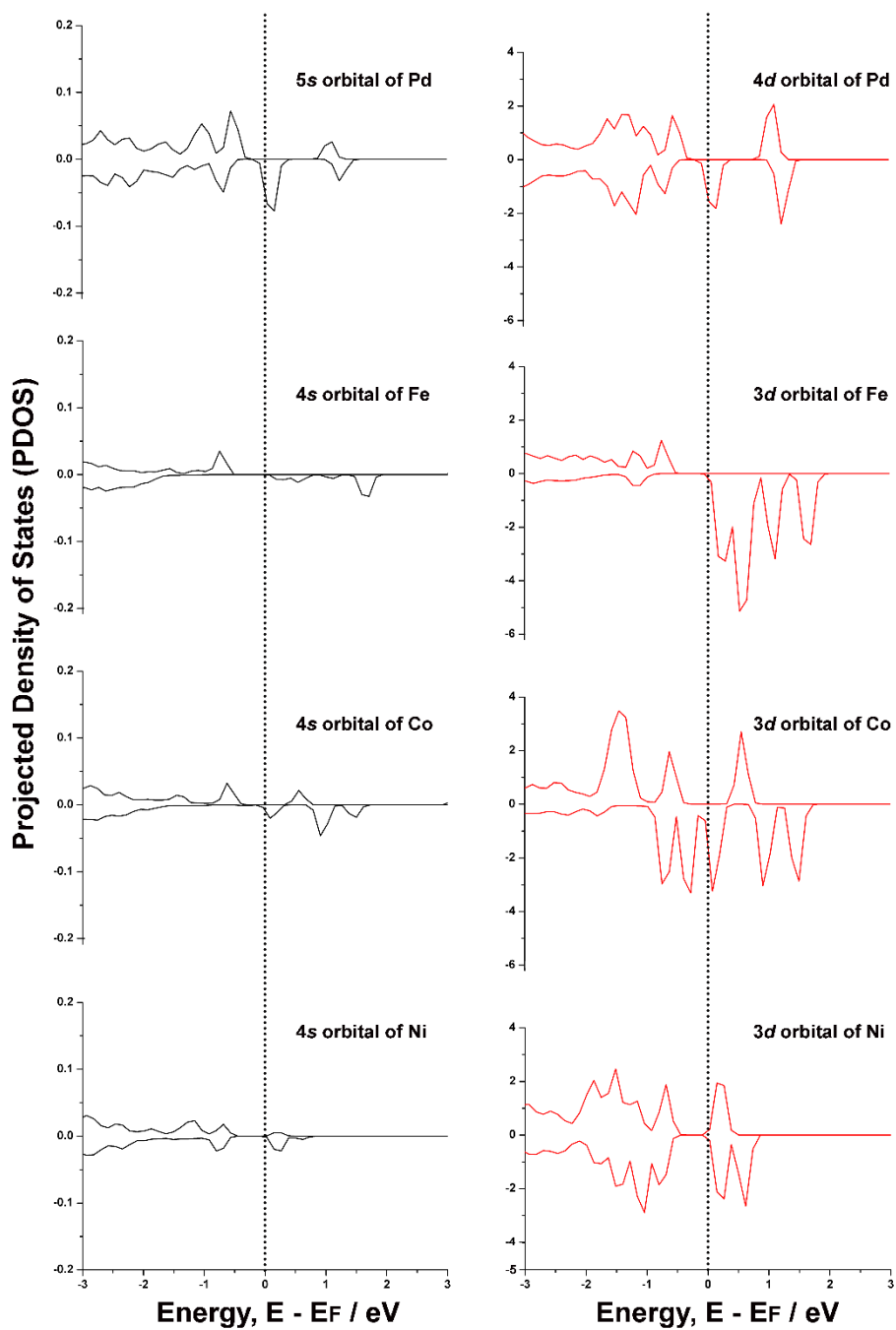


Figure S9. Calculated projected density of states (PDOS) for M-s orbital (left) and M-d orbital (right) of intermediate **8** of $M_1/\text{Al}_2\text{O}_3$ (M = Pd, Fe, Co and Ni).

VII. Geometries and Electronic Properties of Intermediate 9 of M_1/Al_2O_3 ($M = Pd, Fe, Co,$ and Ni)

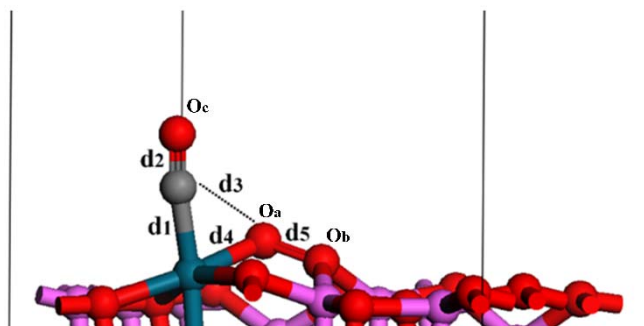


Figure S10. Geometries of intermediate **9** of M_1/Al_2O_3 ($M = Pd, Fe, Co,$ and Ni)

Table S8. Spin state (S), Bader charges of the metal atom (M), two adsorbed oxygen atoms (O_a and O_b), carbon atom (C) and oxygen atom (O_c) of CO atom in intermediate **9**.

System	S	M e	O_a e	O_b e	C e	O_c e
Pd_1/Al_2O_3	0.99	+1.056	-0.362	-0.887	+1.154	-1.046
Fe_1/Al_2O_3	2.99	+1.387	-0.329	-0.886	+1.045	-1.072
Co_1/Al_2O_3	1.78	+1.224	-0.325	-0.855	+1.071	-1.058
Ni_1/Al_2O_3	1.06	+1.161	-0.362	-0.905	+1.111	-1.027

Table S9. Relevant distances in intermediate **9** shown in Figure S10.

System	d_1 Å	d_2 Å	d_3 Å	d_4 Å	d_5 Å
Pd_1/Al_2O_3	1.906	1.148	2.560	1.983	1.443
Fe_1/Al_2O_3	1.839	1.153	2.516	1.849	1.441
Co_1/Al_2O_3	1.780	1.153	2.432	1.815	1.423
Ni_1/Al_2O_3	1.798	1.148	2.385	1.891	1.450

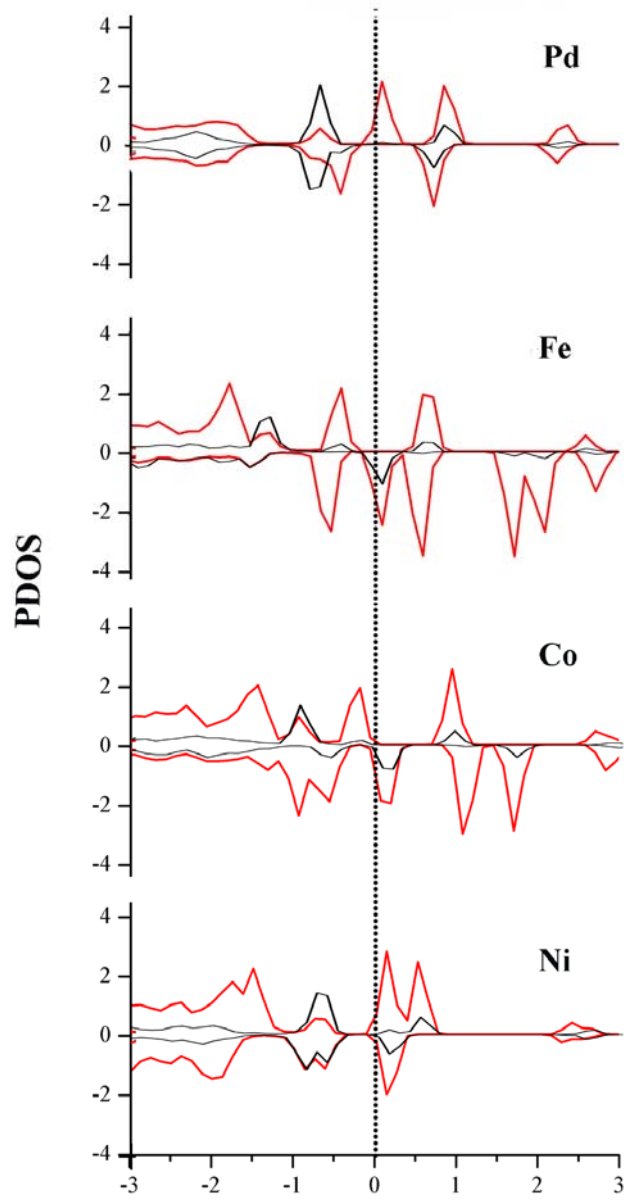


Figure S11. Calculated PDOS for O-*p* orbital (black) and M-*d* orbital (red) in intermediate **9** of M_1/Al_2O_3 ($M = Pd, Fe, Co$ and Ni).